RESEARCH ARTICLE

Evidence for an ABC-Type Riboflavin Transporter System in Pathogenic Spirochetes

Ranjit K. Deka,[a] Chad A. Brautigam,[b] Brent A. Biddy,[b] Wei Z. Liu,[a] Michael V. Norgard[a]

Departments of Microbiology[a] and Biophysics, [b] The University of Texas, Southwestern Medical Center, Dallas, Texas, USA

R.K.D. and C.A.B. contributed equally to this work

ABSTRACT **Bacterial transporter proteins are involved in the translocation of many essential nutrients and metabolites. However, many of these key bacterial transport systems remain to be identified, including those involved in the transport of riboflavin (vitamin B_2). Pathogenic spirochetes lack riboflavin biosynthetic pathways, implying reliance on obtaining riboflavin from their hosts. Using structural and functional characterizations of possible ligand-binding components, we have identified an ABC-type riboflavin transport system within pathogenic spirochetes. The putative lipoprotein ligand-binding components of these systems from three different spirochetes were cloned, hyperexpressed in *Escherichia coli*, and purified to homogeneity. Solutions of all three of the purified recombinant proteins were bright yellow. UV-visible spectra demonstrated that these proteins were likely flavoproteins; electrospray ionization mass spectrometry and thin-layer chromatography confirmed that they contained riboflavin. A 1.3-Å crystal structure of the protein (TP0298) encoded by *Treponema pallidum*, the syphilis spirochete, demonstrated that the protein's fold is similar to the ligand-binding components of ABC-type transporters. The structure also revealed other salient details of the riboflavin binding site. Comparative bioinformatics analyses of spirochetal genomes, coupled with experimental validation, facilitated the discovery of this new ABC-type riboflavin transport system(s). We denote the ligand-binding component as riboflavin uptake transporter A (RfuA). Taken together, it appears that pathogenic spirochetes have evolved an ABC-type transport system (RfuABCD) for survival in their host environments, particularly that of the human host.**

IMPORTANCE **Syphilis remains a public health problem, but very little is known about the causative bacterium. This is because *Treponema pallidum* still cannot be cultured in the laboratory. Rather, *T. pallidum* must be cultivated in laboratory rabbits, a restriction that poses many insurmountable experimental obstacles. Approaches to learn more about the structure and function of *T. pallidum*'s cell envelope, which is both the physical and functional interface between *T. pallidum* and its human host, are severely limited. One approach for elucidating *T. pallidum*'s cell envelope has been to determine the three-dimensional structures of its membrane lipoproteins, molecules that serve many critical survival functions. Herein, we describe a previously unknown transport system that *T. pallidum* uses to import riboflavin, an essential nutrient for the organism's survival. Moreover, we found that this transport system is present in other pathogenic spirochetes. This is the first description of this new type of bacterial riboflavin transport system.**

Received 28 December 2012 **Accepted** 17 January 2013 **Published** 12 February 2013

Citation Deka RK, Brautigam CA, Biddy BA, Liu WZ, Norgard MV. 2013. Evidence for an ABC-type riboflavin transporter system in pathogenic spirochetes. mBio 4(1):e00615-12. doi:10.1128/mBio.00615-12.

Editor E. Peter Greenberg, University of Washington

Address correspondence to Michael V. Norgard, Michael.Norgard@UTSouthwestern.edu.

Treponema pallidum, the causative agent of syphilis, is an obligate spirochetal parasite of humans that remains poorly understood. This primarily is the consequence of the fact that, despite decades of intensive efforts, *T. pallidum* still cannot be cultivated continuously *in vitro* (1). Although complete genome information for *T. pallidum* has been available for almost 15 years (2), many fundamental aspects of the organism's basic physiology, metabolism, and membrane biology remain obscure (3, 4). These information gaps have hindered efforts to understand key mechanistic aspects of the parasitic strategy of this enigmatic human bacterial pathogen.

Although *T. pallidum* has a dual-membrane system, its membrane biology sharply contrasts that of other bacterial diderms. First, *T. pallidum* lacks lipopolysaccharide (LPS) (5), a defining feature of the cell envelope of conventional Gram-negative bacteria (6). Second, its peptidoglycan is not linked to the outer membrane (as in the case of Gram-negative bacteria), but rather the peptidoglycan appears to rest atop a layer likely created by the periplasmic domains of integral cytoplasmic membrane proteins and cytoplasmic membrane-tethered lipoproteins (7, 8). Third, the *T. pallidum* outer membrane has a paucity of outer membrane proteins (2, 3, 9), and only recently have a few bona fide and candidate integral outer membrane proteins been noted (10–13). Recent elegant studies employing cryoelectron tomography have placed these traits into a working model of the molecular architecture of the treponemal cell envelope (7, 8).

Many studies have pointed strongly to the importance of lipoproteins in the overall membrane biology of *T. pallidum* (14, 15).

T. pallidum devotes a large proportion of its limited (~1-Mb) genome to encoding perhaps as many as 48 or more lipoproteins (2, 15), presumably all of which are anchored to the periplasmic leaflets of either the cytoplasmic or outer membranes. In other bacteria, lipoproteins have importance as virulence factors, modular components of ATP-binding cassette (ABC) transporters, nutrient receptors, protective immune targets, proinflammatory agonists, and other effectors (16).

The many enigmatic features of the *T. pallidum* outer envelope raise key questions regarding how the spirochete obtains vital nutrients from its obligate human host. *T. pallidum* likely encodes 39 or so transport proteins, about 60% of which belong to the ABC type transporter family (2, 17). This heavy reliance on transporters likely is a reflection of *T. pallidum*'s inability to synthesize many essential metabolites and components, culminating in the need to exploit its human host by expressing unique transport proteins (18–20). The mechanism(s) by which the parasite acquires and utilizes these essential nutrients can potentially help explain the peculiar membrane biology of *T. pallidum*, elucidate key aspects of its parasitic strategy, and prompt new avenues of investigation for potentially novel antimicrobial drug targets.

Whereas bioinformatics predicts transport proteins in *T. pallidum*, sequence homologies have been unreliable for predicting the functions of these putative treponemal transporters (18, 19, 21). Given the noncultivatable nature of *T. pallidum*, approaches to understand the functions of its proteins have been severely limited. As one approach, we have been exploiting a strategy based on biochemical, biophysical, and bioinformatic studies to garner potential insights into the putative functions of *T. pallidum* membrane lipoproteins. These efforts have led to the elucidation of the functions of several treponemal lipoproteins; some play a major role in nutrient uptake (18–24).

In the current study, structural, biochemical, biophysical, and bioinformatic studies were performed on a recombinant version of the TP0298 lipoprotein, leading to the discovery that TP0298 binds riboflavin (vitamin B_2). Unlike many bacteria, *T. pallidum* cannot synthesize riboflavin, and the mechanism of its acquisition has been unknown. Riboflavin is the essential precursor for flavin adenine dinucleotide (FAD) and flavin mononucleotide (FMN). A crystal structure of TP0298 at a 1.3-Å resolution has elucidated details of the binding site and indicated that the protein belongs to a class of ligand-binding proteins characteristic of ATP-binding cassette (ABC)-type transporters. Because TP0298 is encoded within what appears to be an ABC-type riboflavin uptake (Rfu) transport operon, we have named the protein RfuA, along with its partners (RfuB, RfuC, and RfuD). The components of the RfuABCD transport system are conserved in other spirochetes, suggesting a new type of bacterial ABC-like uptake system for riboflavin.

RESULTS AND DISCUSSION

Expression, purification, and characterization of recombinant proteins. In genomic databases, the *T. pallidum* protein TP0298 is annotated as a "simple sugar transport system substrate-binding protein." However, the primary sequence of TP0298 is 26% identical to that of PnrA, which we have shown binds to purine nucleosides (18). Given this fact, it was initially proposed that TP0298 may also bind a nucleoside. However, upon purification of recombinant TP0298 from *Escherichia coli*, it was immediately obvious that concentrated solutions of TP0298 were bright yellow (not shown), indicating a tightly (possibly covalently) bound chromophore. The UV-visible spectrum of purified recombinant TP0298 showed absorbance maxima around 370 and 450 nm, with a pronounced shoulder at 480 nm (Fig. 1). These absorbance features are known to be associated with flavin-containing compounds (25–27). To assess whether homologs of TP0298 from other pathogenic spirochetes displayed similar traits, we purified two other TP0298-like proteins from *Treponema denticola* and *Borrelia burgdorferi* (TDE0951 and BB_0319, respectively). Solutions containing these proteins were also yellow, and their UV-visible absorbance spectra also demonstrated signature maxima for flavin-containing compounds (Fig. 1).

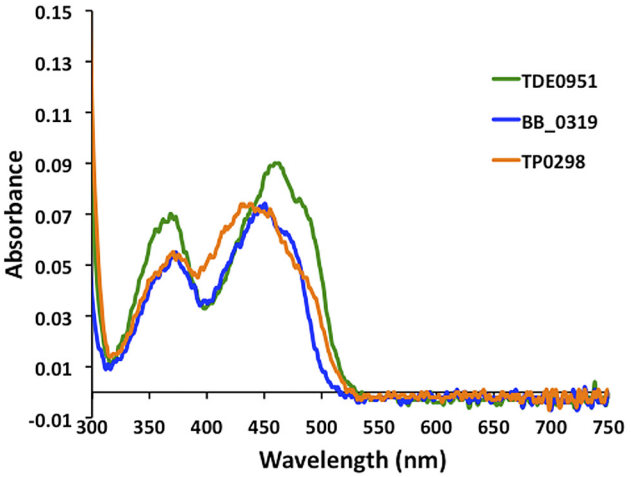

FIG 1 UV-visible spectra of the recombinant TP0298 and related proteins. Correlations between the line colors and protein identities are shown in the legend.

Identification of the bound flavin. Mass spectrometry was performed to identify the putative flavin bound to purified recombinant TP0298. Electrospray ionization mass spectrometry (ESI MS) of this protein under negative ion conditions showed peaks at 38,426 and 376.13 Da (Fig. 2). The calculated mass of the recombinant protein (38,426.9 Da) matched the experimentally determined mass by ESI MS, indicating a noncovalently bound flavin. Examination of the spectrum at lower-mass regions showed a peak with a mass corresponding to that of riboflavin (dissociated from the protein during ionization). The identity of the ligand as a noncovalently bound riboflavin was verified by extracting it from the protein using 0.1% (vol/vol) formic acid and subsequent mass spectrometry (not shown). Using thin-layer chromatography (TLC), we also analyzed the compounds in supernatants after boiling the proteins and removing precipitated protein. As shown in Fig. 3, the chemicals extracted migrated at the same position as the riboflavin standard for all three recombinant proteins studied. The fact that the bound flavin was released either by formic acid extraction (ESI MS) or by boiling (TLC) conclusively indicated that the proteins contained noncovalently bound riboflavin. Because of the copurification of riboflavin and the proteins, we believe that the respective rates of riboflavin dissociation must be very low, likely indicating very high association constants for the protein-riboflavin interactions. Attempts to prepare ligand-free TP0298 for binding studies have not been successful due to its precipitation, indicating that the bound ligand is necessary to maintain the protein's solubility *in vitro*.

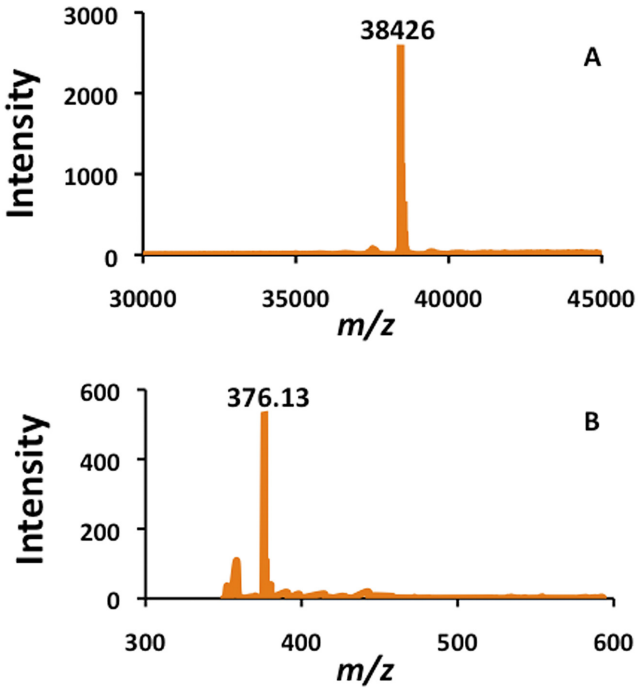

FIG 2 Identification of the flavin bound to recombinant TP0298 by mass spectrometry. (A) Reconstructed ESI MS profiles depicting mass of TP0298 (38,426 Da); (B) profile of released riboflavin during ionization (376.13 Da).

The putative riboflavin ligand-binding protein (TP0298) is encoded within an ABC-type transporter operon. Genomic database annotations of the three riboflavin-containing proteins indicate that they are posited to be ligand-binding proteins (LBPs) of ABC-type transport systems. The architecture of ABC transporters is conserved and typically includes an LBP that specifically recognizes a substrate, an integral membrane permease (forming a pore through which ligand[s] are shuttled into the cytoplasm), and an ATPase (providing the energy for substrate translocation)

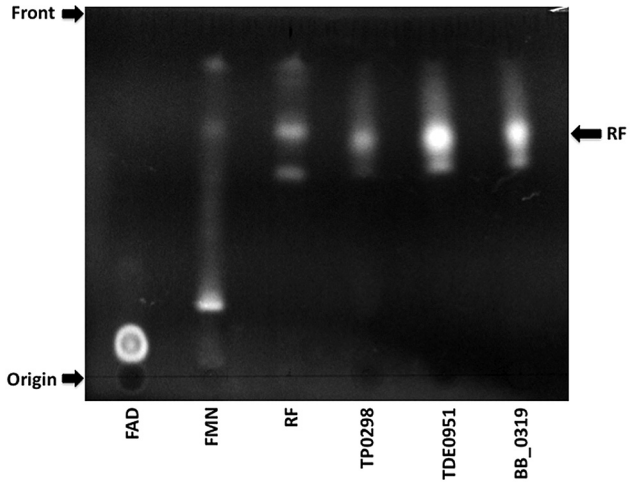

FIG 3 Thin-layer chromatography of bound flavins to recombinant proteins. Flavin standards (FAD, FMN, and riboflavin [RF]) and flavins released from the purified proteins were spotted on the TLC plate, developed, and visualized as described in Materials and Methods.

(28). In bacterial systems, operon structure often reflects a shared biological function among the encoded proteins of coexpressed genes. Genome sequencing indicates that genes *tp0298* to *tp0302* are transcribed from the same DNA strand (but they may not be co-operonic). We hypothesized that the five most downstream genes, *tp0298* (encoding a predicted sugar-binding protein), *tp0299* (encoding a predicted small hypothetical protein), *tp0300* (encoding a predicted ATP-binding protein), *tp0301* (encoding a predicted permease), and *tp0302* (encoding a predicted permease), are part of a putative riboflavin transporter operon in *T. pallidum* (2). Notably, during the course of our investigation, we noticed that there was a sequencing error in the published genomic sequence of *T. pallidum*, resulting in a missing cytidine base at position 3122355. Thus, the division of *tp0299* and *tp0300* into two separate genes is erroneous. Our sequencing of this area confirmed that, indeed, there is only one gene in this region of the genome. We refer to it here as *tp0299/tp0300* to avoid a renumbering of all of the following genes. The amino acid sequence of the corrected gene product did not alter its predicted function as an ATP-binding component of an ABC-type transporter. Our own analyses of the sequences of TP0299/TP0300 to TP0302 comport with the database predictions noted above.

To test the hypothesis that *tp0298* to *tp0302* form a single transcriptional unit, RT-PCR was performed on RNA isolated from rabbit tissue-extracted treponemes using intergenic primers to define the operon and determine its cotranscription. Total DNA and RNA from treponemes were used, and the RT-PCR primers were designed to anneal between the open reading frames (ORFs). Genomic DNA was used as an amplification control, and the cDNA derived from the mRNA was used to detect the transcripts of genes belonging to the putative riboflavin transporter operon. As shown in Fig. 4, all four genes (*tp0298* to *tp0302*) in *T. pallidum* were demonstrated by RT-PCR to be transcriptionally linked, similar to what has been observed for other co-operonic ABC-type transporters (18, 29–31). These results thus confirm the transcriptional hypothesis and suggest that this region forms an operon responsible for riboflavin uptake in *T. pallidum*.

To date, no binding protein-dependent ABC-type transporter for riboflavin has been described for any bacterial system. However, riboflavin (27, 32, 33) is known to be a target for energy coupling factor (ECF) transporters, which are involved in the uptake of vitamins and micronutrients by bacteria (34–37). Unlike ABC-type transporters, ECF-type transporters do not utilize a periplasmic ligand-binding protein. Rather, an integral membrane protein (termed the "S-component") specifically binds the target substrate. Although ABC-type transporters are found in all three domains of life (28), ECF-type transporters are found in prokaryotes only (38). Spirochetes lack ECF-type riboflavin transporters, yet they are auxotrophic for riboflavin (2). Previously, these facts presented a conundrum: how do spirochetes import riboflavin? Our analysis of the TP0298 protein and its respective operon provides the answer to this question: these bacteria employ a heretofore uncharacterized ABC-type riboflavin transporter to acquire this essential nutrient.

Most bacteria synthesize riboflavin *de novo* (39); among those that apparently do not are *Enterococcus faecalis*, *Listeria* species, *Mesoplasma* species, *Rickettsia* species, *Borrelia* species, and *Treponema* species. The putatively auxotrophic strains rely upon transporters to obtain riboflavin from their respective hosts, and, before this study, no ABC-type transporter for flavin acquisition had

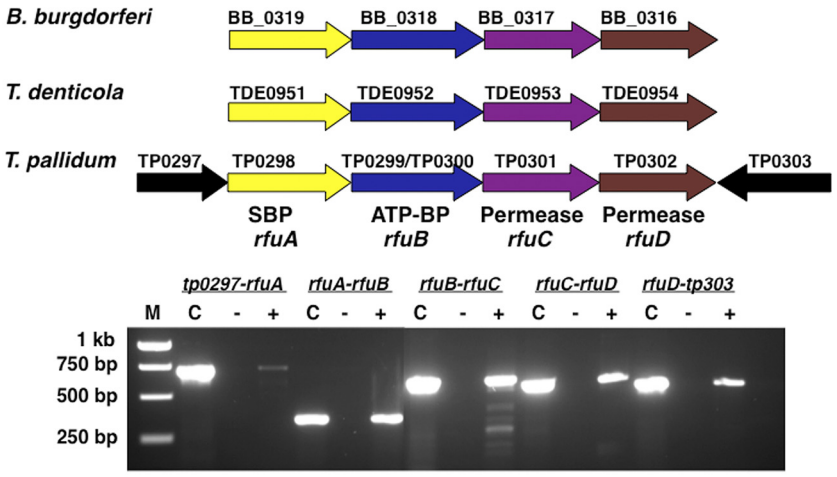

FIG 4 Transcriptional linkage of the putative ABC-type riboflavin transporter operon. Top, schematic representations of the genes as they are organized in the *T. pallidum*, *T. denticola*, and *B. burgdorferi* genomes. RT-PCR was performed on *T. pallidum* RNA using primer pairs, specific for the intergenic regions of listed gene pairs. The lanes for each primer pair are marked as follows: lane C, PCR with indicated primer pair served as positive control using *T. pallidum* genomic DNA as the template in place of cDNA; lane [minus], PCR with indicated primer pair using RNA as the template (lacking RT), which served as a negative control for DNA contamination; lane +, RT-PCR products with the indicated primer pairs; lane M, DNA molecular weight markers. Although RT-PCR of the *tp0297-tp0298* junction did not yield a detectable product, the nonoperonic *tp0302-tp0303* pair did yield a product. This may have been due to the presence of noncoding mRNA that is transcribed in the opposite direction of the *rfu* operon or transcriptional readthrough. Of note, the gel image shown is a composite of two images derived from a single gel. This composite was constructed as a result of removing former reaction products that were observed before the correction of a DNA sequencing error (i.e., former *tp0299* and *tp0300* genes actually are a single [*tp0299/tp0300*] gene; see Results and Discussion).

been identified. Although spirochetes lack the riboflavin biosynthetic pathway, they possess the necessary enzyme (e.g., TP0888 in *T. pallidum*, a predicted FAD synthetase) to generate FMN and FAD cofactors for flavodoxin (TP0925) and other redox enzymes. Thus, the newly identified ABC-type riboflavin transporter likely provides flavin precursors in the cytoplasm for the biosynthesis of FMN/FAD (39).

The contiguous *tp0298* to *tp0302* subset of genes is also conserved in *T. denticola* and *B. burgdorferi* (Fig. 4). It is very likely that these homologous operons are also ABC transporters for riboflavin. ABC transporters typically are named on the basis of the type of ligand bound by the ligand-binding protein (LBP). Because TP0298, TDE0951, and BB_0319 bind riboflavin, we propose renaming these proteins as riboflavin uptake transporter A (RfuA) and the transporter comprising all the components as RfuABCD (Fig. 4). Consequently, we propose to denote the riboflavin uptake operon as the *rfu* operon and the genes encoding the operon as *rfuABCD*. RfuABCD is the first ABC-type operon for riboflavin described in any bacterium.

Oligomeric state of TP0298 and related proteins. Analytical ultracentrifugation sedimentation velocity (SV) experiments were performed to elucidate the oligomerization state of recombinant TP0298. These studies demonstrated that this protein, as purified, is essentially free of contaminants and that it sediments at an experimental *s*-value of 2.8 S (see Fig. S1 in the supplemental material). When the diffusional spread of the solvent/solute boundary is taken into account, an estimate for the molar mass of the protein was 37,100 g/mol. This compares well with the calculated monomeric molar mass (M_c) of the protein construct used in these studies (38,427 g/mol). We therefore conclude that TP0298 is monomeric under the solution conditions employed (see Materials and Methods).

Two related recombinant proteins, BB_0319 and TDE0951, were subjected to similar analyses. The former protein sedimented with an *s*-value of 2.9 S and had an estimated molar mass of 39,500 g/mol (M_c = 39,923 g/mol). Similarly, TDE0951 had an *s*-value of 2.8 S, with an estimated molar mass of 39,300 g/mol (M_c = 38,701 g/mol). Thus, all of the yellow TP0298-like proteins characterized in this study behaved as monomers in solution. Typically, LBPs are monomeric, but there have been reports of similarly structured ligand-binding proteins from tripartite ATP-independent transporters forming dimeric assemblies (40, 41).

Structure of TP0298 and comparison to other LBPs. Recombinant TP0298 was crystallized, allowing its structure to be determined at a resolution of 1.3 Å (see Table S2 in the supplemental material; Fig. 5). Overall, the discernible residues of the protein, 9 to 322 (mature protein numbering), form two lobes that are separated by a cleft. The first lobe (residues 9 to 119, 255 to 279), which we term the "N" lobe because it contains the N terminus of the protein, comprises a six-stranded parallel β-sheet flanked on both sides by α-helices and irregular protein structures. The second lobe (the "C" lobe; residues 121 to 253, 286 to 322) also has a six-stranded β-sheet at its core, but one of the strands is antiparallel to the other five (Fig. 5). Like the N lobe, the C lobe's β-sheet is central and flanked by α-helices and irregular protein structures. There are also three regions of the protein that connect the two lobes: residues 120, 254, and 280 to 285; this last region encompasses a 3_{10} helix. Significantly, the two lobes have structural homology to one another: their 86 comparable C_α atoms have a root mean square difference (RMSD) of 1.9 Å when optimally superposed.

This overall fold is very similar to other LBPs. The overall topology of TP0298 is that of a class I LBP (42), i.e., the first five strands of both β-sheets have the topology β2-β1-β3-β4-β5. In a more recent classification scheme (43), TP0298 falls into cluster B, a group of LBPs that bind to carbohydrates, branched-chain amino acids, peptides, and other small molecules. The connector regions therefore likely collectively serve as a hinge, facilitating

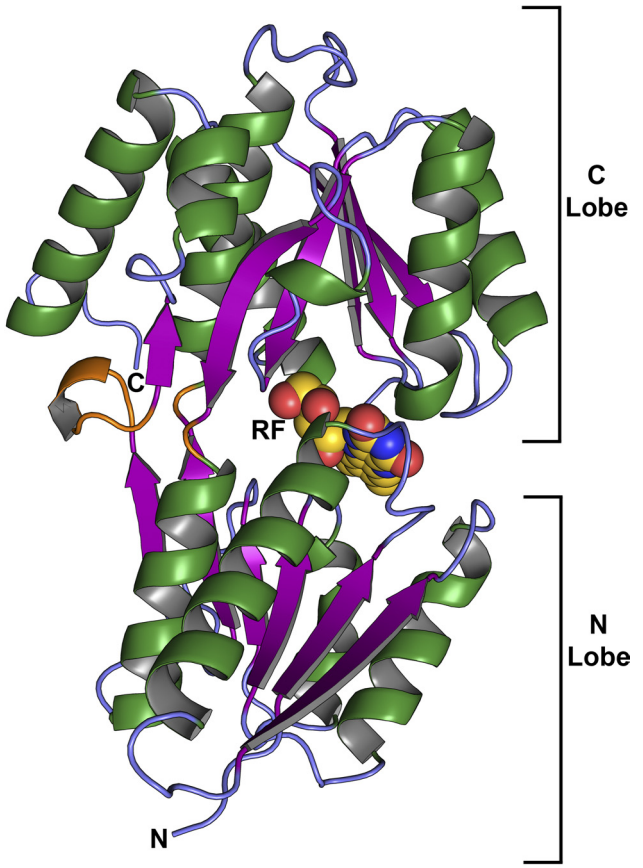

FIG 5 The crystal structure of TP0298. A ribbon-style depiction of the final refined model is shown. The model is colored according to secondary structure: α-helices are green, β-strands are purple, and regions without regular secondary structure are light blue. The exceptions are in the connector regions, which are colored orange. The bound molecule of riboflavin (RF) is shown as a group of spheres; carbon atoms are colored gold, oxygen atoms red, and nitrogen atoms blue. The N and C termini are marked, and the N and C lobes are also labeled.

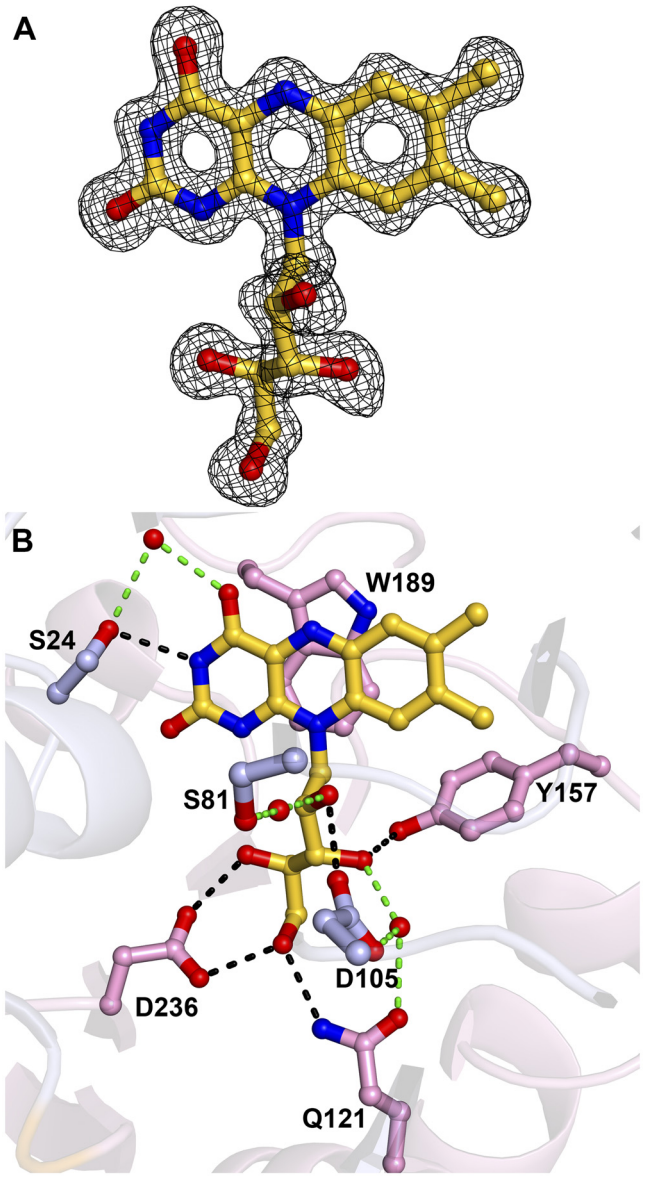

FIG 6 Closeup views of the riboflavin bound to TP0298. (A) Electron density for the riboflavin. Shown is an mF_o-DF_c omit map superposed on the final refined coordinates of the TP0298 model. The map is contoured at the 3 σ level. (B) Contacts between TP0298 and riboflavin. Apparent hydrogen bonds between the riboflavin and TP0298 are shown as black dashes, and apparent hydrogen bonds that are involved in water-mediated contacts between TP0298 and the ligand are shown as green dashes; all distances between atoms shown in this figure are less than 3.0 Å. Atoms are colored as described for riboflavin in Fig. 5, except carbon atoms from the N lobe are colored light blue, and those from the C lobe are pink. Protein secondary structure is shown semitransparently for clarity.

relative movement of the lobes in a "Venus flytrap" motion that is dependent on the liganded state of the protein (44, 45). As noted above, the amino acid sequence of TP0298 is 26% identical to PnrA of *T. pallidum*, which binds purine nucleosides (18). Given their similar primary structures, it is unsurprising that their tertiary structures are also similar; the RMSD of 286 comparable C_α atoms is 1.8 Å after optimal superposition. Structural homology searches using DALI (46) and SSM (47) reveal that TP0298 is homologous to several other LBPs or transcriptional activators: for example, the Med gene product, a transcriptional activator of ComK from *Bacillus halodurans* (48) (RMSD = 1.8 Å over 223 comparable C_α atoms). The mechanism of this transcriptional activator is unknown, but it may bind a small molecule between its two lobes. An adenine-binding protein from *Brucella melitensis* (unpublished PDB accession code 3S99; RMSD = 1.8 Å over 260 comparable C_α atoms) is also structurally similar to TP0298.

Another structure has been determined for a riboflavin-binding component of a riboflavin transporter: that of the ECF-type transporter RibU from *Staphylococcus aureus* (35). However, there is no structural homology between TP0298 and RibU; the latter is a transmembrane protein that contains only α-helices and irregular structural elements. Thus, nature has evolved two very different folds for capturing riboflavin for transport into bacterial cells.

Riboflavin binding by TP0298. In the cleft between the N and C lobes is clear electron density for a single molecule of riboflavin (Fig. 6A). This molecule is included in the TP0298 final model. The ribityl "tail" of the riboflavin is oriented deep within the cleft, approaching the connecting hinge region; the isoalloxazine moi-

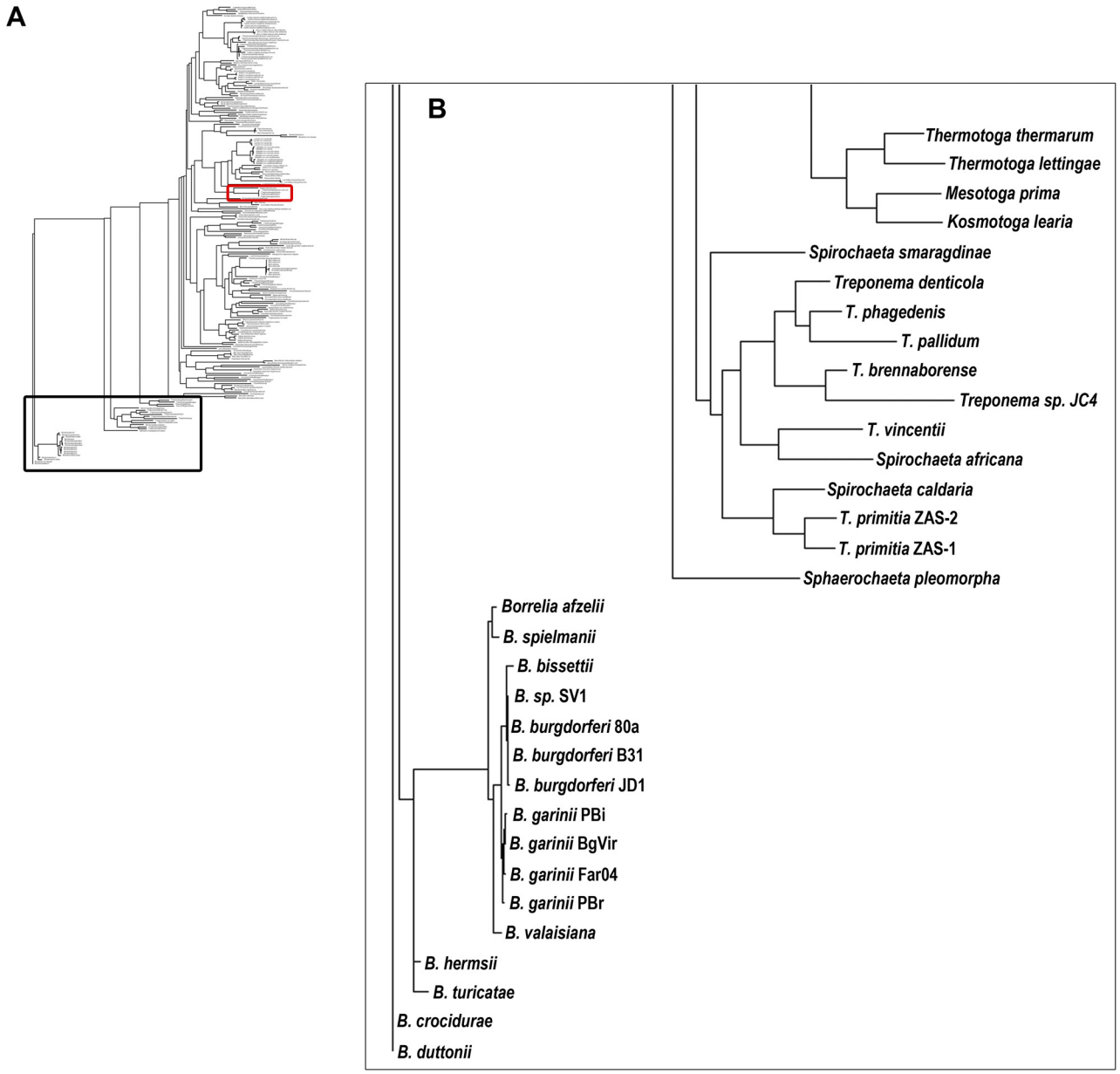

FIG 7 Molecular phylogeny of TP0298-related proteins. (A) A miniaturized phylogram of all 223 proteins. The protein clades most related to TP0298 are outlined in black, while the PnrA-containing clade is outlined in red. (B) A blowup of the phylogeny in the region containing Tp0298.

ety is proximal to the cleft's opening (Fig. 5). Thus, the ribityl moiety is completely buried, but parts of the isoalloxazine moiety (the C7a and C8a methyl groups) are solvent exposed. This observation has an important consequence: the nature of this binding pocket will likely not tolerate decorations on the deeply buried ribityl chain. For example, the addition of a phosphate moiety on the 5′ hydroxyl group of the ribityl chain (forming FMN) would not be compatible sterically or electrostatically with the riboflavin-binding cleft. Therefore, it is very likely that riboflavin alone is the native ligand for TP0298. Indeed, although FMN and FAD are undoubtedly present in the cytoplasm of the expression organism (*E. coli*), only riboflavin is bound to TP0298 (Fig. 2, 3, and 7A).

A complex network of hydrogen bonds and van der Waals interactions is made between the protein and the ligand (Fig. 6B). Some of the contacts between TP0298 and the riboflavin are mediated by water molecules. Notably, the buried ribityl moiety is contacted by charged and polar side chains from the protein, whereas the isoalloxazine ring system mostly interacts with hydrophobic side chains. For example, the indole moiety of W189 is extensively engaged in face-to-face pi-stacking interactions with the *re* face of the isoalloxazine ring of the bound riboflavin. The aromatic portion of Y157 also contacts this *re* face. Stacking on the *si* face (not shown) are the aromatic ring of Y27 (edge to face) and the side chain amide of N82. These mostly hydrophobic contacts are made despite the fact that the isoalloxazine ring has significant

hydrogen-bonding potential. The only direct polar contact between the protein and the ring is O_γ of S24 to N3 of the ring.

The N82 residue is particularly noteworthy in the context of riboflavin binding. The C_β and the amide group of this residue's side chain are no more than 4.0 Å from atoms in the isoalloxazine ring. The main-chain ϕ and ψ angles of N82 combine to make it an outlier in the Ramachandran plot (see Table S2 in the supplemental material). These angles ($\phi = 108.9°$, $\psi = 148.5°$) would make this residue an outlier in the general case, but it is made more so by the fact that N82 precedes a proline residue, P83. According to MolProbity (49), a preproline residue has not been observed to adopt these ϕ and ψ angles in a database of reliably determined crystal structures. We stress that this feature is not due to poor modeling or to a lack of data; the match between the electron density in this region of the protein and the model is excellent, as evidenced by the real-space correlation coefficient of N82 (0.983); also, the side chain of N82 is clearly held in place by hydrogen bonds (2.9 Å). The main-chain nitrogen atom of A84 and the exocyclic oxygen atom of the side chain of Y27 interact with amide oxygen and nitrogen atoms, respectively, of the side chain of N82. Furthermore, the MolProbity analysis of C_β distance deviations (49, 50) demonstrates that N82 is the only residue in the TP0298 model to have such a deviation. It appears that this deviation is forced by the unusual ϕ and ψ angles of this residue that bring the main-chain oxygen atom of S81 into close proximity of C_β of N82. Intriguingly, in PnrA, the residue corresponding to N82 is PnrA-G85 (we here adopt the convention of prefixing residue names with their respective proteins in non-TP0298 cases), and the latter residue has very similar ϕ and ψ angles (120.3°, 150.4°) in its main chain. However, because it is a glycine (i.e., its side chain is a lone hydrogen atom), the strains described above for N82 are absent for PnrA-G85.

As described above, the folds of TP0298 and the riboflavin-binding RibU are very different. However, to deduce any commonalities in their riboflavin-binding strategies, we examined their respective ligand-binding pockets. The riboflavin-binding site of RibU is very different from that of TP0298; the most striking difference is the lack of face-to-face pi-stacking interactions for the isoalloxazine ring bound in the RibU site. Indeed, RibU-Y41 and RibU-F163 have the only aromatic side chains that approach the *re* face of riboflavin bound to RibU, and they approach only the peripheral parts of the ring. We thus conclude that there are very different evolutionary solutions for the binding of riboflavin to the substrate-binding proteins of these two nonhomologous transport systems.

Potential functional relationships among TP0298-like proteins. As noted above, because of their sequence homology to PnrA, proteins in the PnrA/TP0298 family are frequently annotated as "nucleoside-binding proteins" or "PnrA-like." In the broadest sense, both of these predictions are accurate for TP0298; the protein binds a biochemical that resembles a nucleoside in that riboflavin comprises a five-carbon sugar-like moiety and a large, hydrophobic "base" (the isoalloxazine ring). Additionally, it is structurally similar to PnrA (see above). However, such annotations for TP0298 and other riboflavin-binding proteins would overlook a critical aspect of *T. pallidum*'s biology: the organism is auxotrophic for riboflavin, and the proteins TP0298, TP0300, TP0301, and TP0302 are very likely components of an ABC-type transport system for this essential vitamin.

With the goal of more precisely predicting the functions of this family of proteins, we constructed a molecular phylogeny of 223 proteins that were identified as being similar to TP0298 in a BLAST (51) search (PnrA was identified in this search and included in the phylogeny). The three proteins characterized in this report as riboflavin binders are located in two separate clades (Fig. 7). Proteins from treponemes and related spirochetes are in the same clade as TP0298 and TDE0951, whereas BB_0315 is located in a nearby clade that contains proteins from bacteria in the genus *Borrelia*. PnrA and similar proteins are located in a distant clade (Fig. 7A; the full cladogram is shown in Fig. S2 in the supplemental material).

Given this result, which of these clades may be classified as containing riboflavin-binding proteins? Among the amino acids that contact the riboflavin in the TP0298 structure are Y27, N82, Y157, and W189; the equivalent residues in PnrA are different. These residues thus are likely to be predictive for riboflavin binding. In the two clades that are certain to represent riboflavin binders, these residues are strongly conserved. Interestingly, the amino acid at the equivalent of position 27 in *Spirochaeta africana* is glutamate, not tyrosine. However, we consider this to be a conservative substitution, as glutamate may serve the same purposes for riboflavin binding as tyrosine. That is, the methyl groups could provide a hydrophobic surface to pack against the isoalloxazine ring, and the carboxylate group may form a hydrogen bond with the conserved asparagine side chain amide. In a nearby clade containing proteins from the anaerobic genera *Thermotoga*, *Mesotoga*, and *Kosmotoga* (Fig. 7B), three out of these four residues are identical. The one exception is the respective equivalents of N82; these proteins feature threonine at this position. We suspect that the proteins in this clade bind riboflavin. In the next-closest clade, none of these residues is identical to the four discriminatory residues, and, indeed, their chemical characters were closer to those of the corresponding PnrA residues. It seems unlikely that these proteins serve as riboflavin-binding proteins. Thus, only 32 of the 223 TP0298-like proteins that we examined can be hypothesized to be riboflavin binders. This putative binding activity is therefore apparently isolated to a small group of bacteria among spirochetal and anaerobic genera.

Conclusions and implications. An important theme in this structural genomics era is the necessity to verify predicted protein functions through direct experimentation (52). This is particularly the case for treponemal lipoproteins because structural homologies have failed to identify the correct functions of several lipoproteins (18–20). However, experimental verification poses major challenges due to the inability to cultivate and thus genetically manipulate *T. pallidum in vitro* (4). Nonetheless, approaching this problem with spectroscopy, chromatography, bioinformatics, and X-ray crystallography has allowed us to conclude that RfuA is the riboflavin-binding component of a conserved ABC transporter (RfuABCD) in spirochetes. This ABC-type mechanism for riboflavin uptake (shown in Fig. 8) is new and functionally distinct from the ECF-type vitamin transporters. Riboflavin is an essential component of living organisms, being a universal precursor for FMN and FAD coenzymes, which are involved in oxidative metabolism and many other processes (39, 53). Although many microorganisms, as well as plants and fungi, are able to synthesize riboflavin, humans and other animals obtain riboflavin from their diets (54, 55). In the case of *T. pallidum*, where its small (ca. 1-Mb) genome accounts for very limited coding capacity, it is reasonable that the spirochete need not encode what can be sup-

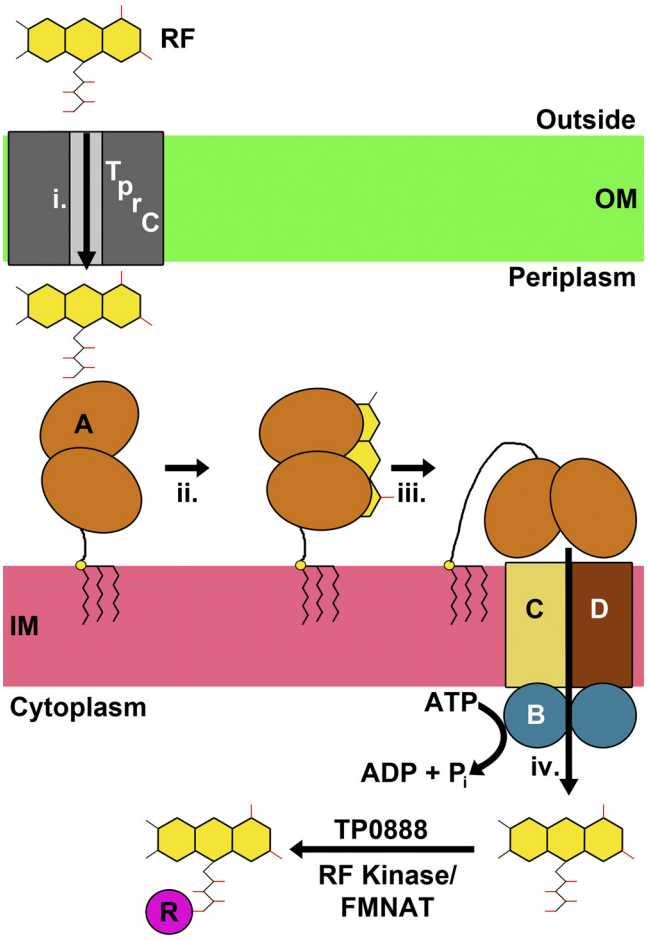

FIG 8 A predicted model regarding the function of RfuABCD transporter. Steps in the proposed model are labeled with lowercase roman numerals, and molecules are labeled with their Rfu designation (A, B, C, or D) or with the locus tag (TP0888). Compounds and proteins are not drawn to scale. Riboflavin (RF) starts on the outside of the cell. By an unknown mechanism (i), perhaps by utilizing an outer membrane porin like TprC, it crosses the outer membrane (OM) to the periplasm. Here, the vitamin is bound by RfuA (ii). In turn, A delivers (iii) the riboflavin to the putative permease-ATPase complex of RfuBCD, which hydrolyzes ATP in order to transport the small molecule into the cytoplasm (iv). Finally, putatively through the action of TP0888, the riboflavin is modified (v). TP0888 is likely a bifunctional enzyme, synthesizing both FMN and FAD; for the former, the group represented by "R" is a phosphate. For FAD, the R group is ADP.

plied by its human host. Furthermore, the biosynthesis of a single riboflavin molecule consumes as many as 25 molecules of ATP (56, 57), making the synthesis of riboflavin energetically costly. Energy conservation must be an important part of the parasitic strategy of this very slow-growing bacterium. Based on histopathological studies, it is widely accepted that *T. pallidum* is an extracellular pathogen (58). The human plasma concentration of riboflavin is ~10 nM (59). Thus, a treponemal riboflavin-binding protein would necessarily have a high affinity for this vitamin. The fact that RfuA can obtain riboflavin when expressed in a heterologous host (*E. coli*) and copurifies with it through several chromatographic procedures is compelling evidence of this high affinity.

T. pallidum is predicted to encode at least one flavoprotein (TP0921) (60), and our current study has revealed three additional flavoproteins (TP0298 [also known as RfuA], TP0888 [also known as FAD synthetase], and TP0925 [also known as flavodoxin]). Although the complete spectrum of flavoproteins in *T. pallidum* remains unknown, it is highly likely that riboflavin plays at least one central role in the physiology, and thus survival, of *T. pallidum* in its human host. *T. pallidum* is believed to lack a functional tricarboxylic acid cycle and cytochromes (4), and thus ATP generation is largely, if not solely, dependent on glycolysis. A pivotal step in the process of ATP generation during treponemal glycolysis is the conversion of NADH to NAD^+ by NADH oxidase (Nox) (TP0921), which requires flavin as a cofactor for converting NADH and O_2 into H_2O (without an H_2O_2 intermediate). Given the need for this Nox-2-like activity in order both to maintain the critical balance of NADH/NAD^+ (and, hence, maintain glycolysis) and for energy generation, the importance of flavin acquisition to the overall biology of *T. pallidum* cannot be overstated. Additional studies on the flavoproteins of *T. pallidum* thus are warranted to expand further our understanding of the even larger impact that flavin utilization likely plays in treponemal physiology and metabolism.

Prior to the current report, nothing was known regarding the mechanism by which essential riboflavin is acquired by *T. pallidum*. A recent study by Anand et al. (10), however, provided evidence to suggest that TprC and TprD are likely outer membrane pore-forming proteins in *T. pallidum*. Riboflavin is a small molecule, so it can either directly diffuse through the treponemal outer membrane or cross through the pore of the newly discovered putative porins. After traversing the outer membrane, it is likely that RfuA serves as the LBP for riboflavin within the periplasm. There, riboflavin binding and transport across the inner membrane via RfuA and its ABC partners (RfuBCD) presumably occurs. Once within the cytoplasm, riboflavin is likely modified to FMN or FAD by FAD synthetase (TP0888) to fulfill the cofactor requirements of the cell (Fig. 8). Importantly, our study provides the first evidence of an ABC-type riboflavin transporter (RfuABCD) in bacteria. These studies also reflect an increased interest in the mechanisms by which obligate bacterial pathogens obtain sequestered riboflavin during human infection and should provide a valuable starting point for the potential development of antimicrobials aimed at preventing the import of this essential nutrient.

MATERIALS AND METHODS

Cloning, overexpression, and protein preparation. To produce a nonlipidated, recombinant derivative of TP0298 in *Escherichia coli*, the DNA fragment encoding amino acid residues 7 to 327 (cloned without the posttranslationally modified N-terminal Cys plus five other hydrophobic residues; the numbering reflects the assignment of this Cys as residue 1 of the processed protein) of TP0298 was PCR amplified from *T. pallidum* genomic DNA using end-specific primers and then ligated into the expression vector pIVEX2.4d vector (5 prime). The resultant plasmid encoded a fusion protein with a His_6 tag at its N terminus. The plasmid was then cotransformed with pGroESL (TaKaRa) into *E. coli* BL21 AI (Invitrogen) cells for soluble protein expression. *E. coli* BL21 AI cells were grown at 37°C in LB medium containing 0.1% (wt/vol) glucose, 100 μg/ml of ampicillin, and 30 μg/ml of chloramphenicol until the cell density reached an A_{600} of 0.5. The culture was then induced at 37°C for 3 h with 0.2% (wt/vol) L-arabinose. For the production of selenomethionine-substituted TP0298 (SeTP0298), the DNA fragment of *tp0298* was cloned into pE-SUMOpro3 bacterial expression vector (LifeSensors), and protein was prepared as described previously (19).

To create soluble, nonlipidated, recombinant versions of proteins ho-

mologous to TP0298, DNA fragments encoding TDE0951 amino acid residues 2 to 326 (cloned without the posttranslationally modified N-terminal Cys residue; the numbering reflects the assignment of this Cys as residue 1 of the processed protein) or BB_0319 residues 29 to 350 (cloned without the first 28 hydrophobic residues; residues 9 to 26 were predicted to be a transmembrane α-helix) were PCR amplified from the respective genomic DNA using end-specific primers and cloned into pProEX HTb expression vectors (Invitrogen). The resultant constructs encoded fusion proteins with His_6 tags at their N termini. Ligation mixtures were transformed into *E. coli* XL1-Blue cells.

E. coli XL1-Blue cells harboring the cloned *tde0951* or *bb_0319* gene fusion were grown at 37°C in LB medium containing 100 μg/ml of ampicillin until the cell density reached an A_{600} of 0.5. Hyperexpression of the recombinant protein was achieved by induction for 3 h with 600 μM IPTG (isopropyl-β-D-thiogalactopyranoside). Cells were harvested and stored at −70°C.

Cell pellets derived from 1 liter of culture were lysed in ice-cold phosphate-buffered saline buffer by sonication. Soluble proteins were purified on an affinity column packed with Ni-nitrilotriacetic acid (NTA) agarose (Qiagen). The proteins were then subjected to size exclusion chromatography using a HiLoad 16/60 Superdex 200 prep-grade column (GE Healthcare) equilibrated with buffer A (20 mM HEPES, 0.1 M NaCl, pH 7.5, 2 mM *n*-octyl-β-D-glucopyranoside). Peak fractions were analyzed by SDS-PAGE. Fractions containing purified proteins were pooled and stored at 4°C in buffer A.

Protein concentration determination and UV-visible absorption spectroscopy. Protein concentrations were determined spectrophotometrically from their extinction coefficients calculated using the ProtParam utility of Expasy (http://us.expasy.org). UV-visible absorption spectra of yellow proteins in buffer A were recorded over the scan range of 300 to 750 nm using a NanoDrop 2000C (Thermo Scientific).

Analytical ultracentrifugation. Centrifugation studies were carried out on preparations of TP0298, TDE0951, and BB_0319 in buffer A at 20°C. After placing the protein solutions (390 μl) in charcoal-filled Epon centerpieces that had been sandwiched between sapphire windows, the centerpieces were sealed and placed in an An50-Ti rotor (Beckman-Coulter). Following that, the samples were equilibrated for 2.5 h under vacuum at the experimental temperature. Finally, the rotor was accelerated to 50,000 rpm, and radial concentration profile data were collected using the absorbance optical system tuned to 280 nm. All analytical ultracentrifugation data were analyzed using the *c*(*s*) methodology (61–63) in the program SEDFIT (www.analyticalultracentrifugation.com. The figure containing the *c*(*s*) analyses was generated in GUSSI (http://biophysics.swmed.edu/MBR/software.html; software authored by C.A.B.).

Thin-layer chromatography analysis. Thin-layer chromatography (TLC) of flavins bound noncovalently to yellow proteins was performed on plates of silica gel (20 cm by 20 cm; thickness, 0.25 mm; pore size, 60 Å; Sigma) plates (64, 65). Protein samples (~100 μM of each) in buffer A were boiled for 10 min and centrifuged to remove protein precipitates. Approximately 20 μl of yellow supernatant was spotted onto the TLC plate. Equal volumes of individual flavin standards were loaded at concentrations of 50 μM. The mobile phase was a solution of butanol-acetic acid-water (12:3:5). The fluorescence of flavin spots on TLC plates was photographed with UV illumination and compared with the flavin standards.

Mass spectrometry. Purified TP0298 in buffer A was prepared in Nanopure water for mass analyses using a Microcon 10-kDa-cutoff filter (Millipore). Under these conditions, protein retained its yellow color. In some experiments, protein samples were extracted with 0.1% (vol/vol) formic acid using the above-described Microcon device. Mass spectra were recorded on a Q-TOF micro mass spectrometer equipped with a nanoelectrospray ion source (Waters-Micromass).

RNA isolation and RT-PCR. Treponemal RNA extraction and RT-PCR methods were described previously (18, 66). The multigene operon was examined by RT-PCR using RNA isolated from *T. pallidum* that had been extracted from rabbit tissue. Intergenic regions were amplified to verify that the genes are cotranscribed in one polycistronic mRNA. cDNA and a control without reverse transcriptase treatment were used as templates. The latter ensured that no chromosomal DNA was carried over into the cDNA preparation. Each RT-PCR reaction was accompanied by a positive-control reaction that utilized the *T. pallidum* genomic DNA to verify the primers. PCR amplification was carried out with GoTaq DNA polymerase (Promega) with a standard protocol and the primers listed in Table S1 in the supplemental material.

Crystallization and structure determination. Crystals of TP0298 were obtained by mixing 3 μl of TP0298 (11 mg/ml) with 3 μl of crystallization buffer (200 mM KSCN, 20% [wt/vol] polyethylene glycol 3350 [PEG 3350]) and incubating them over 0.5 ml of the reservoir for 1 year. These deep-yellow crystals were transferred to the stabilization buffer (SB; 20 mM HEPES [pH 7.5], 0.1 M NaCl, 200 mM KSCN, 22.5% PEG 3350, 5% [vol/vol] ethylene glycol). After about 5 min in SB, they were serially transferred to buffers that were the same as SB except that they had higher concentrations of ethylene glycol. The final ethylene glycol concentration was 25% (vol/vol). After about 1 min in this solution, the crystals were flash-cooled in liquid nitrogen. The crystals diffracted X rays to a minimum *d* spacing of 1.3 Å and exhibited the symmetry of space group $C222_1$. These data were collected at beamline 19-ID in the Structural Biology Center of Argonne National Laboratories. A complete data set at a 1.3-Å resolution was acquired (see Table S2 in the supplemental material). Toward solving the phase problem, crystals of a selenomethionyl derivative of TP0298 (SeTP0298) were grown by the microseeding technique: a crystal of native TP0298 was transferred to SB, which was placed in a microcentrifuge tube. A Teflon bead (Hampton Research) was added, and the tube was vigorously vortexed. This solution was serially diluted, and then 0.5 μl was added to hanging drops of SeTP0298 that had been prepared as described above and allowed to equilibrate for two days. SeTP0298 crystals were apparent within hours after microseeding and were harvested two days after appearing. These crystals were isomorphous to the native TP0298 crystals. A redundant data set was collected (at the beamline mentioned above) using X radiation at a wavelength of 0.97926 Å (see Table S2). Both data sets were processed using HKL2000 (67), utilizing the NO MERGE ORIGINAL INDEX keyword for the SeTP0298 set so that local scaling (68, 69) could be accomplished in subsequent steps. Single-wavelength anomalous diffraction (SAD) protocols available in PHENIX (70) were used to locate heavy-atom sites, refine their parameters, calculate and improve phases, and calculate electron density maps (71, 72). All selenomethionines present in the protein were located using this strategy, except for the N-terminal one. Indeed, the positions of some methionines contributed two sites because of apparent alternate conformations of these residues. RESOLVE (73) was used to automatically build the protein model into the electron density; the program correctly placed 305 out of the 314 amino acid residues that are present in the final model. The initial model was rigid-body refined using the native data set, and then the protocols for simulated annealing, positional, and individual B-factor refinement available in Phenix were used to refine the structure. Anisotropic B-factors were refined. The final model statistics for TP0298 are found in Table S2. Coot (74) was used to manually adjust the model between cycles of refinement. All molecular graphic figures were generated using PyMol (Schrödinger, LLC). The TP0298 structure has been deposited in the Protein Data Bank with the accession code 4IIL.

Bioinformatics. BLAST (51) was used to search for sequence homologs of TP0298. The top 250 hits were compiled; when redundant sequences were removed, 223 sequences remained. Promals 3D (75) was used to align the sequences, using the known crystal structure of PnrA (18) (PDB accession code 2FQW) for structural information. The molecular phylogeny was constructed by PhyML (76) using the LG model of amino acid substitution (77). Archaeopteryx (http://www.phylosoft.org; software authored by C. M. Zmasek) was used to view and output the phylogenetic tree.

SUPPLEMENTAL MATERIAL

Supplemental material for this article may be found at http://mbio.asm.org/lookup/suppl/doi:10.1128/mBio.00615-12/-/DCSupplemental.

Figure S1, PDF file, 0.3 MB.
Figure S2, PDF file, 0.6 MB.
Table S1, PDF file, 0.1 MB.
Table S2, PDF file, 0.1 MB.

ACKNOWLEDGMENTS

We thank Martin Goldberg for technical assistance and the scientists in the UT Southwestern Protein Chemistry Core for protein sequence and mass analyses. We also thank Zhiming Ouyang and Diana R. Tomchick for helpful discussions.

This research was supported by an NIH grant (AI056305-07) to M.V.N. X-ray crystallographic results shown in this report are derived from work performed at Argonne National Laboratory, Structural Biology Center at the Advanced Photon Source. Argonne is operated by UChicago Argonne, LLC, for the U.S. Department of Energy, Office of Biological and Environmental Research, under contract DE-AC02-06CH11357.

REFERENCES

1. **Norris SJ.** 1993. Polypeptides of *Treponema pallidum*: progress toward understanding their structural, functional, and immunologic roles. Microbiol. Rev. **57**:750–779.
2. **Fraser CM, Norris SJ, Weinstock GM, White O, Sutton GG, Dodson R, Gwinn M, Hickey EK, Clayton R, Ketchum KA, Sodergren E, Hardham JM, McLeod MP, Salzberg S, Peterson J, Khalak H, Richardson D, Howell JK, Chidambaram M, Utterback T, McDonald L, Artiach P, Bowman C, Cotton MD, Fujii C, Garland S, Hatch B, Horst K, Roberts K, Sandusky M, Weidman J, Smith HO, Venter JC.** 1998. Complete genome sequence of *Treponema pallidum*, the syphilis spirochete. Science **281**:375–388.
3. **Radolf JD.** 1995. Treponema pallidum and the quest for outer membrane proteins. Mol. Microbiol. **16**:1067–1073.
4. **Norris SJ, Cox DL, Weinstock GM.** 2001. Biology of *Treponema pallidum*: correlation of functional activities with genome sequence data. J. Mol. Microbiol. Biotechnol. **3**:37–62.
5. **Hardy PH, Levin J.** 1983. Lack of endotoxin in *Borrelia hispanica* and *Treponema pallidum*. Proc. Soc. Exp. Biol. Med. **174**:47–52.
6. **Nikaido H.** 2003. Molecular basis of bacterial outer membrane permeability revisited. Microbiol. Mol. Biol. Rev. **67**:593–655.
7. **Liu J, Howell JK, Bradley SD, Zheng Y, Zhou ZH, Norris SJ.** 2010. Cellular architecture of *Treponema pallidum*: novel flagellum, periplasmic cone, and cell envelope as revealed by cryo-electron tomography. J. Mol. Biol. **403**:546–561.
8. **Izard J, Renken C, Hsieh CE, Desrosiers DC, Dunham-Ems S, La Vake C, Gebhardt LL, Limberger RJ, Cox DL, Marko M, Radolf JD.** 2009. Cryo-electron tomography elucidates the molecular architecture of *Treponema pallidum*, the syphilis spirochete. J. Bacteriol. **191**:7566–7580.
9. **Radolf JD, Robinson EJ, Bourell KW, Akins DR, Porcella SF, Weigel LM, Jones JD, Norgard MV.** 1995. Characterization of outer membranes isolated from *Treponema pallidum*, the syphilis spirochete. Infect. Immun. **63**:4244–4252.
10. **Anand A, Luthra A, Dunham-Ems S, Caimano MJ, Karanian C, LeDoyt M, Cruz AR, Salazar JC, Radolf JD.** 2012. TprC/D (Tp0117/131), a trimeric, pore-forming rare outer membrane protein of *Treponema pallidum*, has a bipartite domain structure. J. Bacteriol. **194**:2321–2333.
11. **Desrosiers DC, Anand A, Luthra A, Dunham-Ems SM, LeDoyt M, Eshghi A, Cameron CE, Cruz AR, Salazar JC, Caimano MJ, Radolf JD.** 2011. TP0326, a *Treponema pallidum* β-barrel assembly machinery A (BamA) orthologue and rare outer membrane protein. Mol. Microbiol. **80**:1496–1515.
12. **Cameron CE.** 2006. The *T. pallidum* outer membrane and outer membrane proteins, p 237–266. *In* Radolf JD, Lukehart SA (ed), Pathogenic treponema: molecular and cellular biology. Caister Academic Press, Norfolk, United Kingdom.
13. **Cox DL, Luthra A, Dunham-Ems S, Desrosiers DC, Salazar JC, Caimano MJ, Radolf JD.** 2010. Surface immunolabeling and consensus computational framework to identify candidate rare outer membrane proteins of *Treponema pallidum*. Infect. Immun. **78**:5178–PubMed.
14. **Jones JD, Bourell KW, Norgard MV, Radolf JD.** 1995. Membrane topology of *Borrelia burgdorferi* and *Treponema pallidum* lipoproteins. Infect. Immun. **63**:2424–2434.
15. **Setubal JC, Reis M, Matsunaga J, Haake DA.** 2006. Lipoprotein computational prediction in spirochaetal genomes. Microbiology **152**:113–121.
16. **Kovacs-Simon A, Titball RW, Michell SL.** 2011. Lipoproteins of bacterial pathogens. Infect. Immun. **79**:548–561.
17. **Saier MH, Paulsen IT.** 2000. Whole genome analyses of transporters in spirochetes: *Borrelia burgdorferi* and *Treponema pallidum*. J. Mol. Microbiol. Biotechnol. **2**:393–399.
18. **Deka RK, Brautigam CA, Yang XF, Blevins JS, Machius M, Tomchick DR, Norgard MV.** 2006. The PnrA (Tp0319; TmpC) lipoprotein represents a new family of bacterial purine nucleoside receptor encoded within an ATP-binding cassette (ABC)-like operon in *Treponema pallidum*. J. Biol. Chem. **281**:8072–8081.
19. **Deka RK, Brautigam CA, Goldberg M, Schuck P, Tomchick DR, Norgard MV.** 2012. Structural, bioinformatic, and *in vivo* analyses of two *Treponema pallidum* lipoproteins reveal a unique TRAP transporter. J. Mol. Biol. **416**:678–696.
20. **Brautigam CA, Deka RK, Schuck P, Tomchick DR, Norgard MV.** 2012. Structural and thermodynamic characterization of the interaction between two periplasmic *Treponema pallidum* lipoproteins that are components of a TPR-protein-associated TRAP transporter (TPAT). J. Mol. Biol. **420**:70–86.
21. **Deka RK, Neil L, Hagman KE, Machius M, Tomchick DR, Brautigam CA, Norgard MV.** 2004. Structural evidence that the 32-kilodalton lipoprotein (Tp32) of *Treponema pallidum* is an l-methionine-binding protein. J. Biol. Chem. **279**:55644–55650.
22. **Deka RK, Machius M, Norgard MV, Tomchick DR.** 2002. Crystal structure of the 47-kDa lipoprotein of *Treponema pallidum* reveals a novel penicillin-binding protein. J. Biol. Chem. **277**:41857–41864.
23. **Lee YH, Deka RK, Norgard MV, Radolf JD, Hasemann CA.** 1999. Treponema pallidum TroA is a periplasmic zinc-binding protein with a helical backbone. Nat. Struct. Biol. **6**:628–633.
24. **Machius M, Brautigam CA, Tomchick DR, Ward P, Otwinowski Z, Blevins JS, Deka RK, Norgard MV.** 2007. Structural and biochemical basis for polyamine binding to the Tp0655 lipoprotein of *Treponema pallidum*: putative role for Tp0655 (TpPotD) as a polyamine receptor. J. Mol. Biol. **373**:681–694.
25. **Birch OM, Hewitson KS, Fuhrmann M, Burgdorf K, Baldwin JE, Roach PL, Shaw NM.** 2000. MioC is an FMN-binding protein that is essential for *Escherichia coli* biotin synthase activity in vitro. J. Biol. Chem. **275**:32277–32280.
26. **Ding YH, Ferry JG.** 2004. Flavin mononucleotide-binding flavoprotein family in the domain *Archaea*. J. Bacteriol. **186**:90–97.
27. **Duurkens RH, Tol MB, Geertsma ER, Permentier HP, Slotboom DJ.** 2007. Flavin binding to the high affinity riboflavin transporter RibU. J. Biol. Chem. **282**:10380–10386.
28. **Davidson AL, Dassa E, Orelle C, Chen J.** 2008. Structure, function, and evolution of bacterial ATP-binding cassette systems. Microbiol. Mol. Biol. Rev. **72**:317–364.
29. **Porcella SF, Popova TG, Hagman KE, Penn CW, Radolf JD, Norgard MV.** 1996. A *mgl*-like operon in *Treponema pallidum*, the syphilis spirochete. Gene **177**:115–121.
30. **Hardham JM, Stamm LV, Porcella SF, Frye JG, Barnes NY, Howell JK, Mueller SL, Radolf JD, Weinstock GM, Norris SJ.** 1997. Identification and transcriptional analysis of a *Treponema pallidum* operon encoding a putative ABC transport system, an iron-activated repressor protein homolog, and a glycolytic pathway enzyme homolog. Gene **197**:47–64.
31. **Desrosiers DC, Sun YC, Zaidi AA, Eggers CH, Cox DL, Radolf JD.** 2007. The general transition metal (Tro) and Zn^{2+} (Znu) transporters in *Treponema pallidum*: analysis of metal specificities and expression profiles. Mol. Microbiol. **65**:137–152.
32. **Burgess CM, Slotboom DJ, Eric R, Duurkens RH, Poolman B, Van D, Geertsma ER, Van Sinderen D.** 2006. The riboflavin transporter RibU in *Lactococcus* lactis: molecular characterization of gene expression and the transport mechanism. J. Bacteriol. **188**:2752–2760.
33. **Vogl C, Grill S, Schilling O, Stülke J, Mack M, Stolz J.** 2007. Characterization of riboflavin (vitamin B2) transport proteins from *Bacillus subtilis* and *Corynebacterium glutamicum*. J. Bacteriol. **189**:7367–7375.
34. **Rodionov DA, Hebbeln P, Eudes A, ter Beek J, Rodionova IA, Erkens GB, Slotboom DJ, Gelfand MS, Osterman AL, Hanson AD, Eitinger T.**

2009. A novel class of modular transporters for vitamins in prokaryotes. J. Bacteriol. **191**:42–51.
35. **Zhang P, Wang J, Shi Y.** 2010. Structure and mechanism of the S component of a bacterial ECF transporter. Nature **468**:717–720.
36. **Erkens GB, Berntsson RP, Fulyani F, Majsnerowska M, Vujičić-Žagar A, Ter Beek J, Poolman B, Slotboom DJ.** 2011. The structural basis of modularity in ECF-type ABC transporters. Nat. Struct. Mol. Biol. **18**: 755–760.
37. **Erkens GB, Majsnerowska M, ter Beek J, Slotboom DJ.** 2012. Energy coupling factor-type ABC transporters for vitamin uptake in prokaryotes. Biochemistry **51**:4390–4396.
38. **Eitinger T, Rodionov DA, Grote M, Schneider E.** 2011. Canonical and ECF-type ATP-binding cassette importers in prokaryotes: diversity in modular organization and cellular functions. FEMS Microbiol. Rev. **35**: 3–67.
39. **Fischer M, Bacher A.** 2005. Biosynthesis of flavocoenzymes. Nat. Prod. Rep. **22**:324–350.
40. **Cuneo MJ, Changela A, Miklos AE, Beese LS, Krueger JK, Hellinga HW.** 2008. Structural analysis of a periplasmic binding protein in the tripartite ATP-independent transporter family reveals a tetrameric assembly that may have a role in ligand transport. J. Biol. Chem. **283**:32812–32820.
41. **Gonin S, Arnoux P, Pierru B, Lavergne J, Alonso B, Sabaty M, Pignol D.** 2007. Crystal structures of an extracytoplasmic solute receptor from a TRAP transporter in its open and closed forms reveal a helix-swapped dimer requiring a cation for α-keto acid binding. BMC Struct. Biol. **7**:11.
42. **Fukami-Kobayashi K, Tateno Y, Nishikawa K.** 1999. Domain dislocation: a change of core structure in periplasmic binding proteins in their evolutionary history. J. Mol. Biol. **286**:279–290.
43. **Berntsson RP, Smits SH, Schmitt L, Slotboom DJ, Poolman B.** 2010. A structural classification of substrate-binding proteins. FEBS Lett. **584**: 2606–2617.
44. **Felder CB, Graul RC, Lee AY, Merkle HP, Sadee W.** 1999. The Venus flytrap of periplasmic binding proteins: an ancient protein module present in multiple drug receptors. AAPS PharmSci. **1**:E2.
45. **Mao B, Pear MR, McCammon JA, Quiocho FA.** 1982. Hinge-bending in L-arabinose-binding protein. The "Venus's-flytrap" model. J. Biol. Chem. **257**:1131–1133.
46. **Holm L, Rosenström P.** 2010. Dali server: conservation mapping in 3D. Nucleic Acids Res. **38**:W545–W549.
47. **Krissinel E, Henrick K.** 2004. Secondary-structure matching (SSM), a new tool for fast protein structure alignment in three dimensions. Acta Crystallogr. D Biol. Crystallogr. **60**:2256–2268.
48. **Xu QS, Ankoudinova I, Lou Y, Yokota H, Kim R, Kim SH.** 2007. Crystal structure of a transcriptional activator of comK gene from *Bacillus halodurans*. Proteins **69**:409–414.
49. **Chen VB, Arendall WB, III, Headd JJ, Keedy DA, Immormino RM, Kapral GJ, Murray LW, Richardson JS, Richardson DC.** 2010. Molprobity: all-atom structure validation for macromolecular crystallography. Acta Crystallogr. D Biol. Crystallogr. **66**:12–21.
50. **Davis IW, Leaver-Fay A, Chen VB, Block JN, Kapral GJ, Wang X, Murray LW, Arendall WB, Snoeyink J, Richardson JS, Richardson DC.** 2007. Molprobity: all-atom contacts and structure validation for proteins and nucleic acids. Nucleic Acids Res. **35**:W375–W383.
51. **Altschul SF, Gish W, Miller W, Myers EW, Lipman DJ.** 1990. Basic local alignment search tool. J. Mol. Biol. **215**:403–410.
52. **Strauss EJ, Falkow S.** 1997. Microbial pathogenesis: genomics and beyond. Science **276**:707–712.
53. **Abbas CA, Sibirny AA.** 2011. Genetic control of biosynthesis and transport of riboflavin and flavin nucleotides and construction of robust biotechnological producers. Microbiol. Mol. Biol. Rev. **75**:321–360.
54. **Vitreschak AG, Rodionov DA, Mironov AA, Gelfand MS.** 2002. Regulation of riboflavin biosynthesis and transport genes in bacteria by transcriptional and translational attenuation. Nucleic Acids Res. **30**: 3141–3151.
55. **Macheroux P, Kappes B, Ealick SE.** 2011. Flavogenomics—a genomic and structural view of flavin-dependent proteins. FEBS J. **278**:2625–2634.
56. **Brutinel ED, Gralnick JA.** 2012. Shuttling happens: soluble flavin mediators of extracellular electron transfer in *Shewanella*. Appl. Microbiol. Biotechnol. **93**:41–48.
57. **Bacher A, Eberhardt S, Fischer M, Kis K, Richter G.** 2000. Biosynthesis of vitamin b2 (riboflavin). Annu. Rev. Nutr. **20**:153–167.
58. **Radolf JD, Hazlett KRO, Lukehart SA.** 2006. Pathogenesis of syphilis, p 197–235. *In* Radolf JD, Lukehart SA (ed), Pathogenic treponema: molecular and cellular biology. Caister Academic Press, Norfolk, United Kingdom.
59. **Hustad S, McKinley MC, McNulty H, Schneede J, Strain JJ, Scott JM, Ueland PM.** 2002. Riboflavin, flavin mononucleotide, and flavin adenine dinucleotide in human plasma and erythrocytes at baseline and after low-dose riboflavin supplementation. Clin. Chem. **48**:1571–1577.
60. **Gherardini FC, Boylan JA, Brett PJ.** 2006. Metal utilization and oxidative stress. *In* Radolf JD, Lukehart SA (ed), Pathogenic treponema: molecular and cellular biology. Caister Academic Press, Norfolk, England.
61. **Schuck P, Demeler B.** 1999. Direct sedimentation analysis of interference optical data in analytical ultracentrifugation. Biophys. J. **76**:2288–2296.
62. **Schuck P.** 2000. Size distribution analysis of macromolecules by sedimentation velocity ultracentrifugation and Lamm equation modeling. Biophys. J. **78**:1606–1619.
63. **Schuck P, Perugini MA, Gonzales NR, Howlett GJ, Schubert D.** 2002. Size-distribution analysis of proteins by analytical ultracentrifugation: strategies and application to model systems. Biophys. J. **82**:1096–1111.
64. **Casutt MS, Huber T, Brunisholz R, Tao M, Fritz G, Steuber J.** 2010. Localization and function of the membrane-bound riboflavin in the Na^+-translocating NADH:quinone oxidoreductase (Na^+ NQR) from *Vibrio cholerae*. J. Biol. Chem. **285**:27088–27099.
65. **Herguedas B, Martínez-Júlvez M, Frago S, Medina M, Hermoso JA.** 2010. Oligomeric state in the crystal structure of modular FAD synthetase provides insights into its sequential catalysis in prokaryotes. J. Mol. Biol. **400**:218–230.
66. **Brautigam CA, Deka RK, Ouyang Z, Machius M, Knutsen G, Tomchick DR, Norgard MV.** 2012. Biophysical and bioinformatic analyses implicate the *Treponema pallidum* Tp34 lipoprotein (Tp0971) in transition metal homeostasis. J. Bacteriol. **194**:6771–6781.
67. **Otwinowski Z, Minor W.** 1997. Processing of X-ray diffraction data collected in oscillation mode. Methods Enzymol. **276**:307–326.
68. **Terwilliger TC, Berendzen J.** 1999. Automated MAD and MIR structure solution. Acta Crystallogr. D Biol. Crystallogr. **55**:849–861.
69. **Matthews BW, Czerwinski EW.** 1975. Local scaling: a method to reduce systematic errors in isomorphous replacement and anomalous scattering measurements. Acta Crystallogr. A **31**:480–487.
70. **Adams PD, Afonine PV, Bunkóczi G, Chen VB, Davis IW, Echols N, Headd JJ, Hung LW, Kapral GJ, Grosse-Kunstleve RW, McCoy AJ, Moriarty NW, Oeffner R, Read RJ, Richardson DC, Richardson JS, Terwilliger TC, Zwart PH.** 2010. PHENIX: a comprehensive python-based system for macromolecular structure determination. Acta Crystallogr. D **66**:213–221.
71. **Grosse-Kunstleve RW, Adams PD.** 2003. Substructure search procedures for macromolecular structures. Acta Crystallogr. D Biol. Crystallogr. **59**: 1966–1973.
72. **Terwilliger TC.** 2000. Maximum-likelihood density modification. Acta Crystallogr. D Biol. Crystallogr. **56**:965–972.
73. **Terwilliger TC.** 2003. Automated main-chain model building by template matching and iterative fragment extension. Acta Crystallogr. D Biol. Crystallogr. **59**:38–44.
74. **Emsley P, Cowtan K.** 2004. Coot: model-building tools for molecular graphics. Acta Crystallogr. D Biol. Crystallogr. **60**:2126–2132.
75. **Pei J, Kim BH, Grishin NV.** 2008. PROMALS3D: a tool for multiple sequence and structure alignment. Nucleic Acids Res. **36**:2295–2300.
76. **Guindon S, Dufayard JF, Lefort V, Anisimova M, Hordijk W, Gascuel O.** 2010. New algorithms and methods to estimate maximum-likelihood phylogenies: assessing the performance of PhyML. Syst. Biol. **3** 0:59: 307–321.
77. **Le SQ, Gascuel O.** 2008. An improved general amino acid replacement matrix. Mol. Biol. Evol. **25**:1307–1320.